

Clinical features of patients bearing central nervous system hemangioblastoma in von Hippel-Lindau disease

Hiroshi Kanno · Jun-ichi Kuratsu · Ryo Nishikawa ·
Kazuhiko Mishima · Atushi Natsume ·
Toshihiko Wakabayashi · Kiyohiro Houkin ·
Shunsuke Terasaka · Taro Shuin

Received: 10 July 2012 / Accepted: 25 September 2012 / Published online: 19 October 2012
© Springer-Verlag Wien 2012

Abstract

Background Central nervous system (CNS) hemangioblastoma (HB) is one of the most common manifestations in von Hippel-Lindau disease (VHL), but large-scale studies on clinical features of CNS HB in VHL are scarce.

Methods On the basis of the results of a questionnaire, we collected data of VHL patients with CNS HB.

Results The total number of CNS HBs in 111 VHL patients (male 59, female 52) was 264 with the following distributions: cerebellar, 65.4 %; brainstem, 9.9 %; spinal cord,

23.9 %; and pituitary, 1.1 %. The follow-up period was 0.6 to 39.2 years, with the mean 12.5 years. Patients bearing brainstem or spinal cord HB also had another HB significantly more frequently than those bearing cerebellar HBs ($P < 0.05$). The mean onset age of CNS HB was 29.1 years, and that of patients bearing a single HB (mean 34.4 years) was significantly greater than that of multiple HBs (mean 25.7 years). Patients with multiple HBs under 40 years are more dominant than those with a single HB. The distribution rate of brainstem HB is significantly smaller in patients below 30 years than patients above 29 years. Although ECOG PS score increased along with number of operations, the onset age decreased with increasing number of operations. The mean ECOG PS score of patients below 20 years is significantly smaller than patients above 19 years.

Conclusions When the onset age of CNS HB is under 40 years, and CNS HB is located at the brainstem or spinal cord HB, the probability of multiple occurrence can be predicted. Since patients with an onset age under 20 years old preserve a high performance status, early detection of CNS HB would be important. In addition, since a multiple operations aggravate performance status, number of operations should be reduced.

H. Kanno (✉)
Department of Neurosurgery, Yokohama City University
School of Medicine,
3-9 Fukuura,
Kanazawa-ku, Yokohama 236-0004, Japan
e-mail: hiroshikannomd@nifty.com

J.-i. Kuratsu
Department of Neurosurgery, Kumamoto University
School of Medicine,
Kumamoto, Japan

R. Nishikawa · K. Mishima
Department of Neurosurgery, Saitama Medical University,
Hidaka, Japan

A. Natsume · T. Wakabayashi
Department of Neurosurgery, Nagoya University
Graduate School of Medicine,
Nagoya, Japan

K. Houkin · S. Terasaka
Department of Neurosurgery, Hokkaido University
Graduate School of Medicine,
Sapporo, Japan

T. Shuin
Department of Urology, Kochi University School of Medicine,
Nangoku, Japan

Keywords Central nervous system hemangioblastoma ·
Von Hippel-Lindau disease · Clinical features · Quality of life

Introduction

Von Hippel-Lindau disease (VHL) is a familial neoplasia disorder with an autosomal dominant pattern of inheritance that results from a germline mutation in the *VHL* gene, and which is characterized by a predisposition to develop

multiple neoplastic lesions, including central nervous system (CNS) hemangioblastomas (HBs), retinal HBs, renal cell carcinomas (RCCs), pheochromocytomas (PhCs), pancreatic tumors (PTs), endolymphatic sac tumors (ELSTs), and epididymal cystadenomas (ECs) [9, 11–13]. VHL gene, located at chromosome 3p25 region, was isolated by a positional cloning approach [7] and shown to be mutated in the germline of VHL patients, as well as in sporadic tumors including CNS HBs [5] and RCCs [16]. Common CNS lesions in affected individuals include cerebellar, spinal cord, brainstem HBs, as well as retinal HBs, pituitary stalk HBs, and ELSTs [3, 4, 8–10, 13]. The annual incidence of VHL is approximately one in 36,000 live births and has over 90 % penetrance by 65 years of age [9, 11–13]. The earliest feature among manifested lesions in VHL patients is usually a retinal or cerebellar HB. At present, metastases from RCC and neurological complications from CNS HBs are the most common causes of death. Although the median survival of VHL patients previously did not reach 50 years, the prognosis of VHL patients has been improved and the complications related to VHL-associated lesions were reduced by comprehensive serial screening and routine follow-up, earlier diagnosis of lesions in VHL patients by computed imaging and laboratory studies including DNA tests, progress in treatment such as microsurgery or radiotherapy for CNS HB and tumor enucleation for RCC, and increased knowledge of VHL [9]. At present, even small asymptomatic HBs in VHL patients are detected on an MRI without difficulty [11]. Since most VHL patients with a CNS HB also have other CNS HBs and/or visceral tumors, these patients might have opportunities to undergo treatment for other CNS HBs or visceral tumors in the future. Large-scale epidemiological studies involving over 100 patients have rarely been done, and the clinical features of CNS HBs in VHL disease are not yet fully defined. In addition, the previous studies mostly have treated a smaller number of only cerebellar or spinal cases; and therefore the clinical aspects and the quality of life of CNS HBs in VHL patients have not yet been fully elucidated [1, 17]. Here, focusing particularly on onset age of CNS HB, we describe the clinical features and quality of life of HBs in the CNS of VHL patients.

Materials and methods

VHL patients were gathered by the Japanese VHL Study Group in the Japanese Health & Labor Ministry during 2009–2010 via the results of a questionnaire (Table 1) answered by Japanese neurosurgeons at 1020 hospitals approved as training facilities for neurological surgery in Japan. The clinical diagnosis for VHL was made on the basis of the following criteria [9]. In the

presence of a positive family history, VHL can be diagnosed clinically in a patient with at least one typical VHL tumor, retinal or CNS HB; RCC; PhC; and PT. ELSTs and multiple pancreatic cysts suggest a positive carrier. In contrast, in patients with a negative family history of VHL-associated tumors, diagnosis of VHL can be made when they exhibit two or more CNS HB or a single HB in association with a visceral tumor such as RCC, PhC, and PT. All CNS HBs or visceral tumors were diagnosed on the basis of clinical histories, symptoms, histories, laboratory studies, and radiological findings made by CT or MR. Among the collected VHL patients, those bearing CNS HBs were investigated with respect to the following: patients' characteristics, location of CNS HB, onset age of CNS HB, follow-up period, number of operations for CNS HB, and radiation therapy. In addition, performance status (PS) at the point based on the results of the questionnaire was assessed according to the following Eastern Cooperative Oncology Group (ECOG) PS [14]. The relationship between the number of operations and the PS or onset age of CNS HB was also examined. Exclusion criteria were as follow: incomplete description about location of tumor, onset age or performance status. For statistical analysis, we applied the non-parametric Mann-Whitney's *U* test or Spearman's correlation coefficient rank test. Statistical significance was set at $P < 0.05$. This study was conducted with the approval of the ethics committee of Kochi University School of Medicine which is the center of this study.

Results

According to the criteria described in the Methods section, 294 patients were defined as VHL according to results of the questionnaire. Among them, 200 (68.1 %) bore CNS HBs. Among these 200 patients, their tumor locations, onset age, ECOG PS, and follow-up period were clarified in 111 patients. Summary of data on CNS HBs in VHL patients is shown in Table 2. Among 111 patient, 2 died due to CNS HB at 44 and 47 years, and remaining 109 patients were living.

Among the 111 patients bearing CNS HBs, those bearing cerebellar ones were 92 (82.9 %); brainstem, 22 (20.7 %); spinal cord, 43 (38.7 %); pituitary, 3 (2.7 %). Fifty-three patients had only cerebellar HBs (30, single tumor; 23, multiple ones). Ten patients had only spinal cord HB (seven, single tumor; three, multiple ones); and three patients had only brainstem HBs (two, single tumor; one, multiple ones). In addition, the result of the present study revealed that 83.7 % of the patients with spinal cord HB had another CNS HB at

Table 1 Questionnaire on central nervous system hemangioblastoma (CNS HB) in VHL

Onset age of CNS HB		() years old or the Year ()						
Times of therapy	Age	() years old		<input type="checkbox"/>	tumor removal			
	or	the Year		<input type="checkbox"/>	stereotactic radiotherapy			
The first time	()	()		<input type="checkbox"/>	external irradiation			
	Location	()		<input type="checkbox"/>	other therapy			
	<input type="checkbox"/>	cerebellum						
	<input type="checkbox"/>	brainstem						
	<input type="checkbox"/>	spinal cord	<input type="radio"/>	C(cervical)	<input type="radio"/>	T(thoracic)	<input type="radio"/>	L/S(lumbosacral)
	() years old	()		<input type="checkbox"/>	tumor removal			
The second time	or	the Year		<input type="checkbox"/>	stereotactic radiotherapy			
	()	()		<input type="checkbox"/>	external irradiation			
	Location	()		<input type="checkbox"/>	other therapy			
	<input type="checkbox"/>	cerebellum						
	<input type="checkbox"/>	brainstem						
	<input type="checkbox"/>	spinal cord	<input type="radio"/>	C(cervical)	<input type="radio"/>	T(thoracic)	<input type="radio"/>	L/S(lumbosacral)
The third time and following	() years old	()		<input type="checkbox"/>	tumor removal			
	or	the Year		<input type="checkbox"/>	stereotactic radiotherapy			
	()	()		<input type="checkbox"/>	external irradiation			
	Location	()		<input type="checkbox"/>	other therapy			
	<input type="checkbox"/>	cerebellum						
	<input type="checkbox"/>	brainstem						
	<input type="checkbox"/>	spinal cord	<input type="radio"/>	C(cervical)	<input type="radio"/>	T(thoracic)	<input type="radio"/>	L/S(lumbosacral)

ECOG Performance Status		
Check	Score	definition
<input type="radio"/>	0	Full active, able to carry on all pre-disease performance without restriction.
<input type="radio"/>	1	Restricted in physically strenuous activity but ambulatory and able to carry out work of a light or sedentary nature.
<input type="radio"/>	2	Ambulatory and capable of all self-care but unable to carry out any work activities. Up and about more than 50% of working hours.
<input type="radio"/>	3	Capable of only limited self-care, confined to bed or chair more than 50% of working hours.
<input type="radio"/>	4	Completely disabled. Cannot carry on any self-care. Totally confined to bed or chair.
<input type="radio"/>	5	dead

the same and/or another site; and, similarly, 91.3 % of the patients with brainstem HB also had another CNS HB at the same and/or another site, and 68.4 % of the patients with cerebellar HBs had CNS HB at the same and/or another site (Fig. 1). The distribution of 63 spinal cord HBs is as follows: cervical, 50.6 %; thoracic, 37.0 %; lumbar, 12.3 %. The number of patients

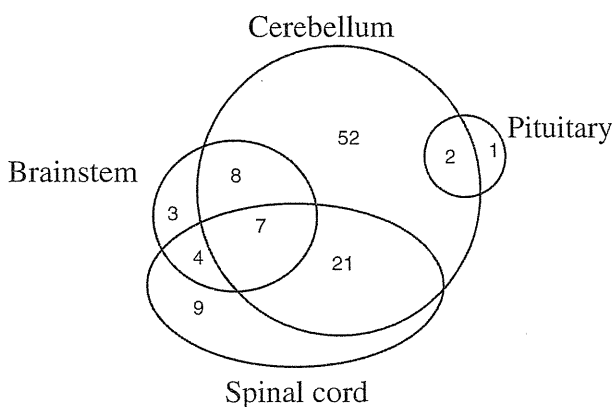
having undergone radiotherapy was 10, and all radiotherapies were performed with stereotaxic radiosurgery. In VHL patients below 40 years old, patients bearing multiple HBs are more dominant than those bearing single HB, while in VHL patients above 39 years old, those bearing single HB are more dominant than those bearing multiple HBs. The distribution rate of brainstem HB is

Table 2 Summary of data on CNS hemangioblastomas (HBs) in VHL patients

Characteristics	
Male/female	59/52
VHL patients with treated CNS HBs	108
VHL patients with untreated CNS HBs	3
Onset age of CNS HB (mean years±s.d.)	7 to 73 (29.1±12.6)
VHL patients with a single HB	34.4±15.8
VHL patients with multiple HBs	25.7±9.8
Period of follow-up (mean years±s.d.)	0.6 to 39.2 (12.5±9.3)
ECOG Performance status (PS) (mean score±s.d.)	0.77±1.16
ECOG PS 0	63 (56.8 %)
ECOG PS 1	29 (26.1 %)
ECOG PS 2	8 (7.2 %)
ECOG PS 3	6 (5.4 %)
ECOG PS 4	3 (2.7 %)
ECOG PS 5	2 (1.8 %)
Distribution of all CNS HBs	264
Cerebellum	172 (65.2 %)
Spinal cord	63 (23.9 %)
Brainstem	26 (9.8 %)
Pituitary	3 (1.1 %)
Distribution of onset CNS HBs in VHL patients	111
Cerebellum	79 (71.2 %)
Spinal cord	21 (18.9 %)
Brainstem	10 (9.0 %)
Pituitary	1(0.9 %)
Total number of operation	251
Times of operation per patient (mean times±s.d.) 1 to 9	1 to 9 (2.2±1.8)

significantly higher in patients below 30 years old than patients above 29 years old ($P<0.01$) (Table 3).

The onset age of VHL patients with a single HB (34.4±15.4 years) was significantly higher than the patients with

**Fig. 1** Distribution of CNS HBs in 111 VHL patients

multiple HBs (25.7±12.6 years) ($P<0.001$). Similarly, the mean onset age of patients bearing a single cerebellar HB (33.8 ±15.0 years) was significantly higher than that of patients bearing multiple cerebellar HBs and/or HBs at another site (26.2 ±8.9 years). Likewise, in the case of patients bearing a single spinal cord HB, this mean age (35.9 ±17.5 years) was significantly higher than that of patients bearing multiple spinal cord HBs and/or HBs at another site (24.4 ±12.1 years old) ($P<0.01$). Patients bearing multiple HBs are more dominant than those bearing single HB in patients below 40 years old, while those bearing single HB are significantly more dominant than those bearing multiple HBs in patients above 39 years old ($P<0.01$) (Table 3).

ECOG PS was assessed based on the results of the questionnaire. Those patients having low ECOG PS scores ($PS=0, 1$) were 82.9 %, while higher ECOG PS scores ($PS\geq 2$) were 17.1 % of the total 111 patients. The relationship between ECOG PS score and the onset age of CNS HB showed a tendency that patients having a lower PS score were at a lower onset age, but there was no significant correlation ($P=0.06$). The mean ECOG PS score of patients below 20 years old was significantly smaller than patients above 19 years old ($P<0.01$). The mean ECOG PS of patients with a single CNS HB (0.34±0.76) was significantly lower than that of patients with multiple CNS HBs (0.87±1.14) ($P<0.005$). In addition, the mean ECOG PS of patients bearing cerebellar HB was 0.67±1.04, and the mean ECOG PS of patients bearing a single cerebellar HB (0.24±0.69) was significantly lower than that of patients bearing multiple cerebellar HBs and/or HBs at another site or single cerebellar HB with HB at another site (0.87±1.12, $P<0.005$). The mean ECOG PS of patients bearing a spinal cord HB was 0.88±1.1. The mean ECOG-PS of patients bearing spinal cord HB was 0.88±1.1, and that of those bearing a single spinal cord HB (0.69±0.95) was not significantly lower than that of patients bearing multiple spinal cord HBs and/or HBs at another site HB or a single spinal cord HB with an HB at another site (0.93±1.20, $P=0.46$). ECOG PS score of VHL patients bearing a single CNS HB is significantly smaller than that of those bearing multiple CNS HBs in all onset age groups ($P<0.05$).

Among 111 VHL patients, 108 patients underwent a total of 251 operations, while the remaining three patients did not undergo treatment for CNS HB. All three patients with untreated CNS HB were above 39 years old, with a mean of 42.7 years old. Among these three patients with untreated CNS HB, two have one cerebellar HB and one has two CNS HBs (cerebellum, 1 and spinal cord, 1). ECOG PS scores of patients with untreated HBs were as follows: two patients, PS 0; and one, PS 4. The follow-up period of patients with untreated HB ranged from 1 to 7 years (mean 5 years). On the other hand, the number of

Table 3 Onset age of CNS HB and other clinical features

Onset age of CNS HB (years)	-19 (N=26)	20–29 (N=41)	30–39 (N=24)	40- (N=20)
Male/Female	11/15	26/15	14/10	9/11
Single/Multiple	7/19	17/24	8/16	15/5
Follow-up period	13.54±9.14	13.61±8.92	13.54±10.87	7.5±6.81
Total number of CNS HB	75	103	62	24
Mean number of CNS HB	2.88±1.97	2.51±1.80	2.58±1.86	1.2±0.52
Distribution of all CNS HB	C47/B12/S15/P1	C58/B12/S33/P1	C52/B1/S9	C15/B1/S6/P1
Distribution of onset CNS HB	C19/B2/S4/P1	C28/B6/S7	C18/B1/S5	C14/B1/S5
Total number of operations	67	101	63	20
Mean number of operations	2.58±1.94	2.46±1.83	2.63±1.95	1±0.65
Mean ECOG PS score	0.29±0.46	0.73±1.11	0.83±1.34	0.89±1.18
ECOG PS score single	0	0.5±1.03	0.13±0.35	0.77±1.17
ECOG PS score multiple	0.41±0.51	0.88±1.15	1.19±1.51	1.2±1.3

operations per patient with treated CNS HBs ranged from 1 to 9, with a mean of 2.2 ± 1.8 . In the first operation, cerebellar HB was dominant; but in the second operation, the rate of the spinal cord HB operation increased. In the spinal cord operations for HB, the first and third operations were dominantly performed at the cervical level, while the second operation was dominantly at the thoracic one (Fig. 2). As to the relationship between number of operations and ECOG PS, the ECOG PS score significantly increased together with the operation number ($P<0.001$). In contrast, in the relationship between operation number and onset age of CNS HB (Fig. 3), the latter significantly decreased with increasing number of operations ($P<0.005$); with a mean of 32.9 years for one operation; a mean of 26.2 years for two operations; and a mean of 23.9 years

for three and more operations. As to the relationship between number of operations and onset age of CNS HBs, the mean numbers of CNS HB and operation for CNS HB in onset age of VHL patients above 39 years old are significantly smaller than other onset age groups ($P<0.05$) (Table 3, Fig. 3).

Discussion

Approximately two-thirds of CNS HBs are sporadic in origin, while the remaining third are associated with VHL. HBs in the CNS are a common feature in VHL patients, and are often also accompanied by such lesions at other sites, although sporadic CNS HBs are almost always universally solitary. Approximately two-thirds of VHL patients bear

Fig. 2 Sites of CNS HBs with respect to operation number are shown. **a** Cerebellar HBs were always the most dominant, while spinal cord and brainstem HBs were always the second and the third, respectively. The proportion of spinal cord HBs increased with operation number, particularly in the second operation. **b** Number of spinal cord HBs with respect to spinal cord level and operation number. In the first operation, the cervical level was the most dominant location; whereas in the second, the thoracic was the most dominant one. In the third and fourth operations, the cervical level was the most dominant

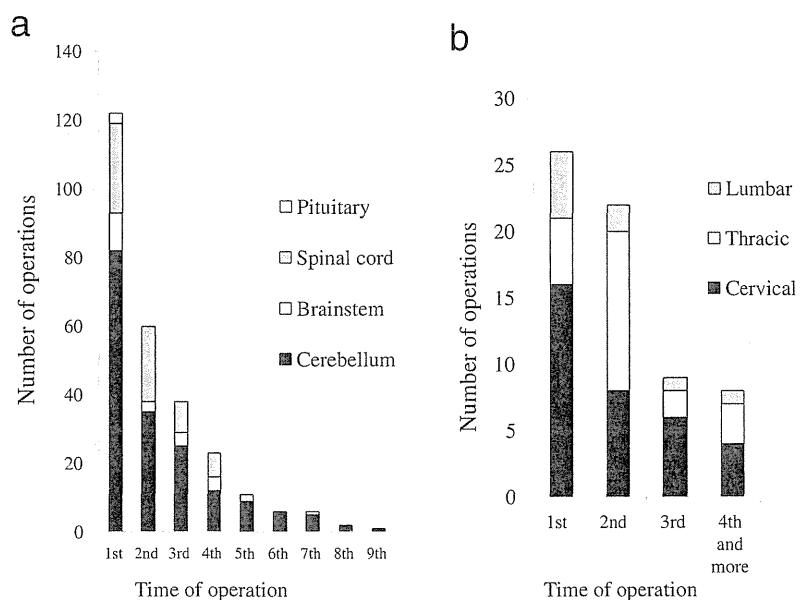
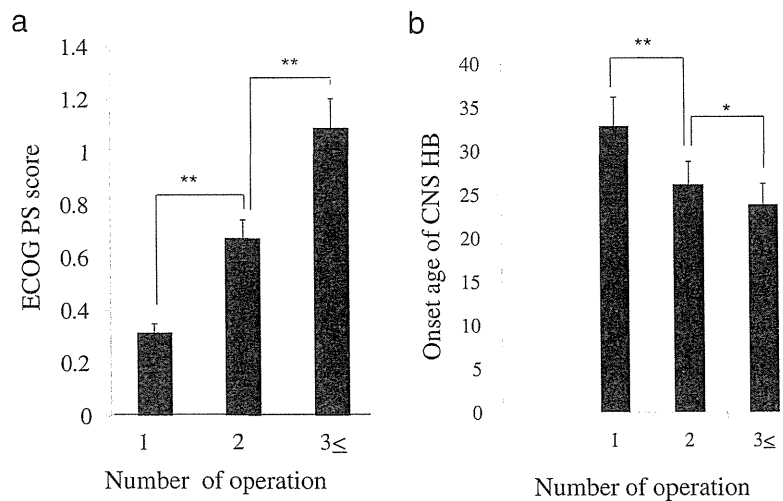


Fig. 3 Relationship between number of operation and ECOG performance status (PS) score or onset age of CNS HB is shown. **a** The ECOG PS score was significantly positively correlated with the number of operations. **b** Relationship between number of operation and onset age (years) of CNS HB is inversely correlated with number of operation. ** $P < 0.01$, * $P < 0.05$



CNS HBs; and among these HBs, cerebellar are the most dominant, and spinal cord ones are next, with brainstem HBs being third [12, 13, 15]. Another frequently found site is the pituitary [16]. In contrast, such lesions in the cerebral intraparenchymal region or intraventricular region are rare. These frequently found regions match those in which hematopoietic embryonic stem cells reside [17]. The HB distribution in this present study is similar to that found in previous studies [1–3, 12, 13].

Spinal cord HB or brainstem HB is frequently also associated with an HB at some other site, mostly cerebellar HB; whereas cerebellar HB is less frequently associated with HBs at other locations [14]. These findings suggest that spinal cord or brainstem HB is usually accompanied by cerebellar HB and that cerebellar HB is often an independent pathology. In other words, when a spinal cord HB or a brainstem HB is found in a patient, such a patient should be predicted to have another manifested lesion associated with VHL, particularly a CNS HB; and this possibility should be explored.

Our present study showed that the ECOG performance status score was positively correlated with the number of operations and with the onset age of CNS HB. VHL patients frequently undergo multiple operations for CNS HBs, but multiple operations aggravate performance status. If possible, the number of operation for CNS HBs should be reduced. The present study showed that the first operation was mostly for cerebellar HB and that there was an increase in the proportion of spinal cord HB, particularly thoracic, at the second operation. This change in proportion from the first operation to the second one would be expected to affect performance status. When a CNS HB is identified, and the patient is diagnosed as VHL at an age under 40 years, we can thus predict that another HB will appear in the CNS in the future, particularly in brainstem or spinal cord HB. In contrast, when a CNS HB is identified in the cerebellum and the patient is diagnosed as

VHL over 39 years of age, we can predict that another CNS HB will not appear later. Our present study also showed that a single HB was different from multiple HBs in terms of onset age of CNS HB and performance status. The onset age of CNS HB in VHL patients bearing a single HB was significantly older than that for VHL patients bearing multiple HBs. This present study showed that VHL patients will probably have only a single HB when the onset age of CNS HB is over 39 years, but that they will have multiple HBs under the onset age of 40 years. This result indicates that scheduled follow-up is necessary if onset age is under 40 years but that it is not always necessary if onset age is above 39 years. In addition, the present study also showed that the ECOG PS score of patients below 20 years old was significantly smaller than that of patients above 19 years old. This result suggests that early detection of CNS HB in VHL patients and annually follow-up is important, and that thereby the annual follow-up may provide patients opportunities to undergo adequate treatment and may contribute to preserve a high performance status of patients. However, further studies are required to confirm the findings of this study, because the number of VHL patients bearing CNS HB above 39 years or below 20 years are small in this study.

Conclusion

When the onset age of CNS HB is under 40 years and CNS HB is located in brainstem or spinal cord, the probability of multiple occurrence of CNS HBs can be predicted and close scheduled follow-up is necessary. We would emphasize that since the onset age under 20 years old patients preserve high performance status, early detection of CNS HB in VHL patients and annually follow-up would be important, and that since multiple operations aggravate performance status in VHL patients, number of operations had better be reduced.

Acknowledgments This work was supported by a grant-in-aid for scientific research No. 228 from the Ministry of Health and Labor of Japan.

Conflict of interest None.

References

1. Ammerman JM, Lonser RR, Dambrosia J, Butman JA, Oldfield EH (2006) Long-term natural history of hemangioblastomas in patients with von Hippel-Lindau disease: implications for treatment. *J Neurosurg* 105:248–255
2. Colombo N, Kucharczyk W, Brant-Zawadzki M, Norman D, Scotti G, Newton TH (1986) Magnetic resonance imaging of spinal cord hemangioblastoma. *Acta Radiol Suppl* 369:734–737
3. Conway JE, Chou D, Clatterbuck RE, Brem H, Long DM, Rigamonti D (2001) Hemangioblastomas of the central nervous system in von Hippel-Lindau syndrome and sporadic disease. *Neurosurgery* 48:55–63
4. Filling-Katz MR, Choyke PL, Oldfield E, Charnas L, Patronas N, Glenn G, Gorin M, Morgan J, Linehan W, Seizinger B, Zbar B (1991) Central nervous system involvement in Von Hippel-Lindau disease. *Neurology* 41:41–46
5. Kanno H, Kondo K, Ito S, Yamamoto I, Fujii S, Trigo S, Sakai N, Hosaka M, Shuin T, Yao M (1994) Somatic mutations of the von Hippel-Lindau tumor suppressor gene in sporadic central nervous system hemangioblastomas. *Cancer Res* 54:4845–4847
6. Kanno H, Yamamoto I, Nishikawa R, Matsutani M, Wakabayashi T, Yoshida J, Shitara N, Yamasaki I, Shuin T, Clinical VHL Research Group in Japan (2009) Spinal cord hemangioblastomas in von Hippel-Lindau disease. *Spinal Cord* 47
7. Latif F, Tory K, Gnarr J, Yao M, Duh FM, Orcutt ML, Stackhouse T, Kuzmin I, Modi W, Geil L, Schmidt L, Zhou F, Li H, Wei MH, Chen F, Glenn G, Choyke P, Walther MM, Weng Y, Duan DR, Dean A, Glavac D, Richards FM, Crossey PA, Ferguson-Smith MA, Le Paslier D, Chumakov I, Cohen D, Chinault CA, Maher ER, Linehan WM, Zbar B (1993) Identification of the von Hippel-Lindau disease tumor suppressor gene. *Science* 260:1317–1320
8. Lonser RR, Butman JA, Kiringoda R, Song D, Oldfield EH (2009) Pituitary stalk hemangioblastomas in von Hippel-Lindau disease. *J Neurosurg* 110(2):350–353
9. Lonser R, Glenn GM, Walther M, Chew EY, Libutti SK, Linehan WM, Oldfield EH (2003) Von Hippel-Lindau disease. *Lancet* 361:2059–2067
10. Neumann HP, Eggert HR, Scheremet R, Schumacher M, Mohadjer M, Wakhloo A, Volk B, Hettmannsperger U, Riegler P, Schollmeyer P, Wiestler O (1992) Central nervous system lesions in von Hippel-Lindau syndrome. *J Neurol Neurosurg Psychiatry* 55:898–901
11. Neumann HP, Lips CJ, Hsia YE, Zbar B (1995) Von Hippel-Lindau syndrome. *Brain Pathol* 5:181–193
12. Maher ER, Kaelin WG Jr (1997) von Hippel-Lindau disease. *Medicine (Baltimore)* 76:381–391
13. Maher ER, Yates JR, Harries R, Benjamin C, Harris R, Moore AT, Ferguson-Smith MA (1990) Clinical features and natural history of von Hippel-Lindau disease. *Q J Med* 77:1151–1163
14. Oken MM, Creech RH, Tormey DC, Horton J, Davis TE, McFadden ET, Carbone PP (1982) Toxicity and response criteria of the Eastern Cooperative Oncology Group. *Am J Clin Oncol* 5:649–655
15. Park DM, Zhuang Z, Chen L, Szerlip N, Maric I, Li J, Sohn T, Kim SH, Lubensky IA, Vortmeyer AO, Rodgers GP, Oldfield EH, Lonser RR (2007) von Hippel-Lindau disease-associated hemangioblastomas are derived from embryologic multipotent cells. *PLoS Med* 4:333–341
16. Shuin T, Kondo K, Torigoe S, Kishida T, Kubota Y, Hosaka M, Nagashima Y, Kitamura H, Latif F, Zbar B, Lerman M, Yao M (1994) Frequent somatic mutations and loss of heterozygosity of the von Hippel-Lindau tumor suppressor gene in primary human renal cell carcinoma. *Cancer Res* 54:2852–2855
17. Wanebo JE, Lonser RR, Glenn GM, Oldfield EH (2003) The natural history of hemangioblastomas of the central nervous system in patients with von Hippel-Lindau disease. *J Neurosurg* 98:82–94

Article

Isolation of Multipotent Nestin-Expressing Stem Cells Derived from the Epidermis of Elderly Humans and TAT-VHL Peptide-Mediated Neuronal Differentiation of These Cells

Hiroshi Kanno ^{1,*}, Atsuhiko Kubo ¹, Tetsuya Yoshizumi ¹, Taro Mikami ² and Jiro Maegawa ²

¹ Department of Neurosurgery, Yokohama City University, Yokohama 236-0004, Japan;
E-Mails: kubstar@msj.biglobe.ne.jp (A.K.); yoshizumi316@tea.ocn.ne.jp (T.Y.)

² Department of Plastic Surgery, Yokohama City University, Yokohama 236-0004, Japan;
E-Mails: zeong3@mac.com (T.M.); maegawaj@med.yokohama-cu.ac.jp (J.M.)

* Author to whom correspondence should be addressed; E-Mail: hiroshikannomd@nifty.com;
Tel.: +81-45-787-2663; Fax: +81-45-783-6121.

Received: 7 March 2013; in revised form: 17 April 2013 / Accepted: 23 April 2013 /
Published: 3 May 2013

Abstract: A specialized population of cells residing in the hair follicle is quiescent but shows pluripotency for differentiating into epithelial-mesenchymal lineage cells. Therefore, such cells are hoped to be useful as implantable donor cells for regenerative therapy. Recently, it was reported that intracellular delivery of TAT-VHL peptide induces neuronal differentiation of skin-derived precursors. In the present study, we successfully isolated multipotent stem cells derived from the epidermis of elderly humans, characterized these cells as being capable of sphere formation and strong expression of nestin, fibronectin, and CD34 but not of keratin 15, and identified the niche of these cells as being the outer root sheath of the hair follicles. In addition, we showed that TAT-VHL peptide induced their neuronal differentiation *in vitro*, and confirmed by fluorescence immunohistochemistry the neuronal differentiation of such peptide-treated cells implanted into rodent brains. These multipotent nestin-expressing stem cells derived from human epidermis are easily accessible and should be useful as donor cells for neuronal regenerative cell therapy.

Keywords: hair follicle; multipotent stem cells; nestin; neuronal differentiation

1. Introduction

The epidermis in humans is a multilayered epithelium composed of hair follicles, sebaceous glands, and interfollicular epidermis between the orifices of the hair follicles [1]. A specialized nestin-positive cell population residing in the hair follicle has the self-renewing capacity to form spheres and has the potential as multipotent stem cells to differentiate into cells of not only the epithelial lineage, but also mesenchymal lineage [2]. This specialized cell population is located in the upper, middle, and lower parts of hair follicles in mice [3], whereas it resides in the outer root sheath of hair follicle below the sebaceous glands in humans [2,4]. The cells in this population are also referred to as epidermal neural crest stem cells [5], and are similar to hair follicle dermal papilla stem cells [6], termed skin-derived precursors (SKPs) [7]. It has been suggested that the major source of hair follicle stem cells originate from the hair follicle bulge region [8,9], and nascent blood vessels in the skin were shown to arise from these cells [10]. Recently, non-invasive high-resolution multiphoton tomography was used to observe living cells [11], and by it follicle stem cells were seen to traffic from the hair bulge area towards the dermal papilla [12]. In addition, this population of cells contains both multipotent and monopotent stem cells [13], the both of which are capable of becoming epidermal stem cells [14]; and also SKPs derived from hair follicle stem cells exhibit properties of adult dermal stem cells [15]. The pluripotency of hair follicle stem cells is suggested to be related to epithelial-mesenchymal cross-talk [1]. Markers of cells obtained from human epidermis are keratin 15 and $\alpha 6$ -intergrin; whereas CD34 is expressed in the outer root sheath below the bulge region in human hair follicles, though it is highly expressed in the bulge region in mice [16]. Cell markers of human nestin-expressing hair follicle stem cells include nestin and fibronectin but not keratin 15 [16,17]. Previously, nestin-expressing follicle stem cells in adult humans were reported [2,18,19], but hair follicle stem cells obtained from elderly humans over 70 years have never been reported. In addition, both fibronectin and CD34 have never been simultaneously examined as stem cell markers.

Human skin is an attractive source of somatic pluripotent stem cells such as hair follicle stem cells or hair follicle dermal papilla stem cells due to easy access to them. It has been reported that implantation of multipotent nestin-positive hair follicle stem cells promotes the repair of spinal cord and peripheral nerves [8,20–22]. Intractable neuronal diseases such as Parkinson's disease and numerous other intractable diseases are mostly found in elderly patients. However, little has yet been reported on the isolation of stem cells obtained from the skin of elderly humans. Previously we demonstrated that von Hippel-Lindau tumor suppressor protein (pVHL) induces neuronal differentiation of neuronal progenitor cells [23], and recently, the intracellular delivery of a peptide consisting of amino-acids corresponding to the elongin BC binding site within pVHL into skin-derived precursors, neural stem cells, and bone marrow stromal cells was reported to result in their neuronal differentiation [24–27].

Here we show the isolation of nestin-expressing stem cells from elderly human epidermis and the neuronal differentiation of these cells when VHL-peptide was delivered into them. In addition, we show that these nestin-expressing stem cells simultaneously expressed fibronectin and CD34 but not keratin 15, and identify the niche of these cells as being the outer root sheath of hair follicles. Furthermore, these somatic stem cells implanted into rodent brains were confirmed to be positive for neuronal markers.

2. Results

2.1. Isolation and Characterization of Multipotent Nestin-Expressing Stem Cells Derived from the Epidermis of Elderly Patients

Facial skin samples were obtained from 16 elderly patients having a complaint of ptosis, which is symptomatically the downward positioning or drooping of the upper eye-lid that occurs with aging, prior to plastic surgery. The patients (6 males and 10 females) ranged in age from 55 to 86 years with a mean age of 69.1 ± 9.5 years, and seven patients were over 70 years of age (the oldest patient, 86 years). Samples of the surplus skin removed at surgery for ptosis were used for this study. The epidermis, rich in hair follicles, was peeled off from the dermis after dispase treatment. Then, the epidermis was cut into small fragments, digested with trypsin, and filtered through a 40- μm -pore cell strainer. After having been dissociated into single cells, the epidermal cells were cultured in medium consisting of DMEM/F12 containing B27 supplement, basis fibroblast growth factor, and epidermal growth factor, but no serum. The cells were observed under a phase-contrast microscope every 3–4 days starting one day after the establishment of the primary cultures. The stem cells among them started to form spheres one week after the start of the primary cultures, and these spheres grew little by little (Figure 1A). By 4 weeks numerous spheres were found floating in the culture medium (Figure 1B). Although the sphere formation, being a reflection of self-renewal capacity, was recognized as having been due to these stem cells, the cell growth became slower after the fourth week (Figure 1C). Among the cells dissociated from spheres in six-weeks-primary cultures, $78.3\% \pm 12.1\%$ of them were positive for nestin; $83.1\% \pm 11.5\%$, positive for fibronectin; and $72.3\% \pm 10.3\%$, positive for CD34. In contrast, only $9.3\% \pm 1.4\%$ of them showed expression of keratin 15; and only $8.7\% \pm 1.2\%$, that of NGFP p75 (Figure 2D). One week after dissociation of these sphere-forming cells, the single cells cultured in medium consisting of DMEM/F12 medium containing 1% fetal calf serum without growth factors or supplement differentiated into neuron-marker (microtubule-associated protein, MAP)-2-positive cells (Figure 2E), astrocyte-marker (glial fibrillary acidic protein, GFAP)-positive cells (Figure 2F) or smooth muscle marker (smooth muscle actin, SMA) -positive cells (Figure 2G).

2.2. Niche of Multipotent Nestin-Expressing Stem Cells Derived from Epidermis of Elderly Humans

In our pathological analysis of elderly human whole skin including both epidermis and dermis, the niche of nestin-expressing stem cells derived from the epidermis was identified to be the outer root sheath region of the hair follicles, which cells showed high triple expressions of nestin, fibronectin, and CD34 (Figure 3A,B). On the other hand, high expression of keratin 15 was detected in both the follicle and the interfollicle regions (Figure 3C). Thus the location of the triple (nestin, fibronectin, and CD34)-expressing cells was different from that of the keratin 15-expressing ones. Except for the bulge region, some of the dermal tissue beneath the epidermis contained a population of cells immunopositive for these triple markers. In addition, in the pathological analysis of the epidermis only (Figure 3D), the sites of nestin and keratin 15 were completely different. These results suggested that the niche of nestin-expressing cells was the outer root sheath of the hair follicles.

Figure 1. (A) One week after the start of a primary culture of cells derived from the epidermis from an elderly human. Sphere formation was recognized; (B) Four-week-old primary culture. Numerous floating spheres were observed; (C) Results from a sphere-forming assay. After 4 weeks, the rate of sphere formation became slow. Scale bars = 50 μ m.

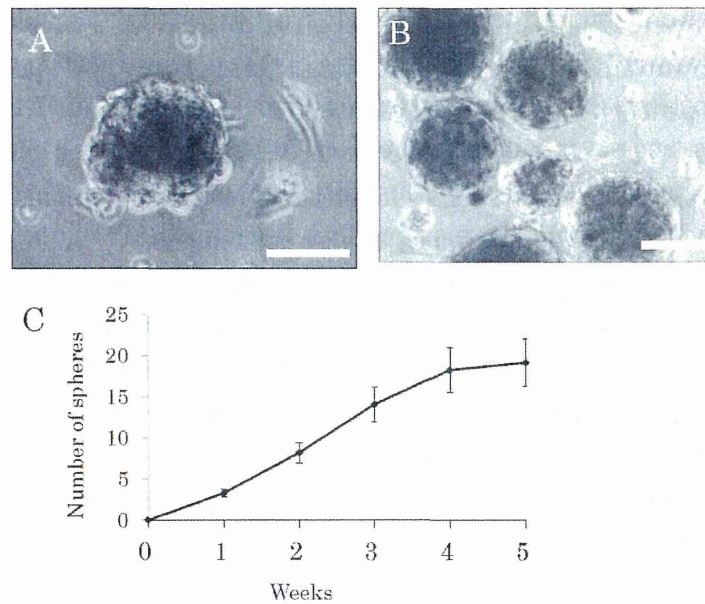


Figure 2. Fluorescence immunocytochemistry of the cultured stem cells after dissociation of the spheres into single cells. The spheres at 5 weeks in primary culture were dissociated by pipetting. (A) Triple fluorescence immunocytochemistry for expressions of CD34 (green) and fibronectin (red) and visualization of nuclei (blue); (B) Triple fluorescence immunocytochemistry for nestin (green), NGFR p75 (red), and nuclei (blue); (C) Triple fluorescence immunocytochemistry for nestin (green), keratin 15 (red), and nuclei (blue); (D) Percentages of the cells showing expression of the five proteins examined. High expressions of nestin, fibronectin, and CD34 were found, whereas those of keratin 15 and NGFR p75 were low. DAPI, nuclear marker; Merge, all three images superimposed; (E–G) Fluorescence immunocytochemical study on differentiation of stem cells into neurons expressing microtubule-associated protein (MAP)-2 (green, E), astrocytes expressing glial fibrillary acidic protein (GFAP; green, F), and smooth muscle cells expressing smooth muscle actin (SMA; green, G), with the nucleus in blue. Scale bars = 50 μ m.

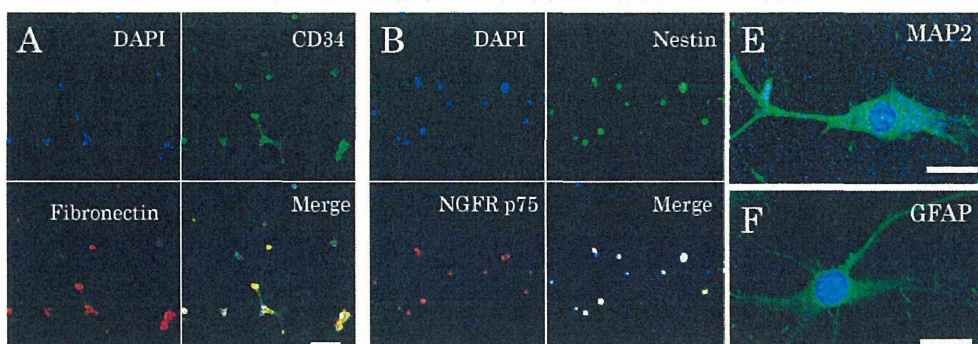


Figure 2. Cont.

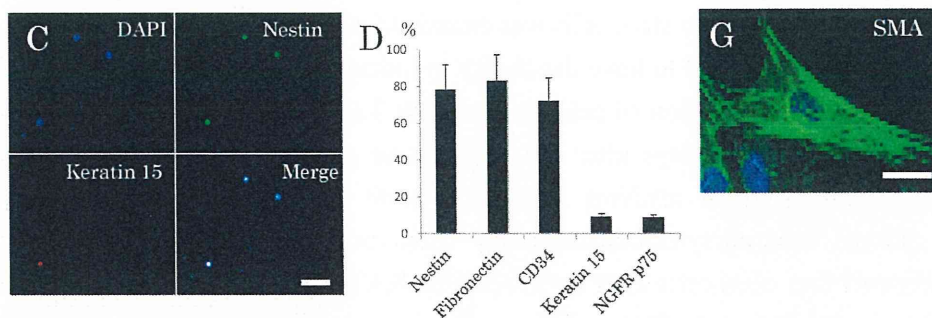
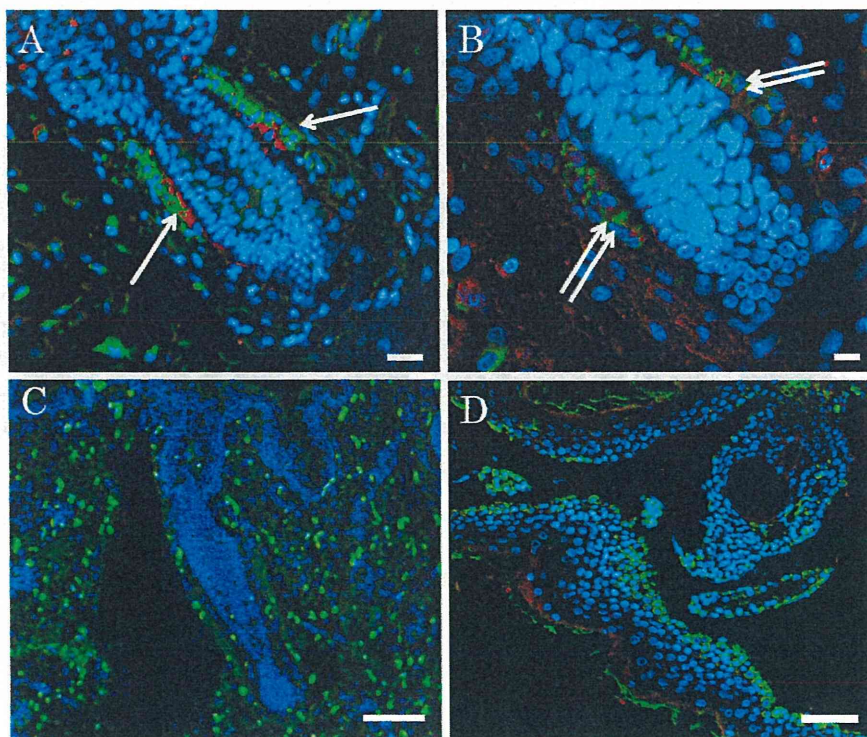


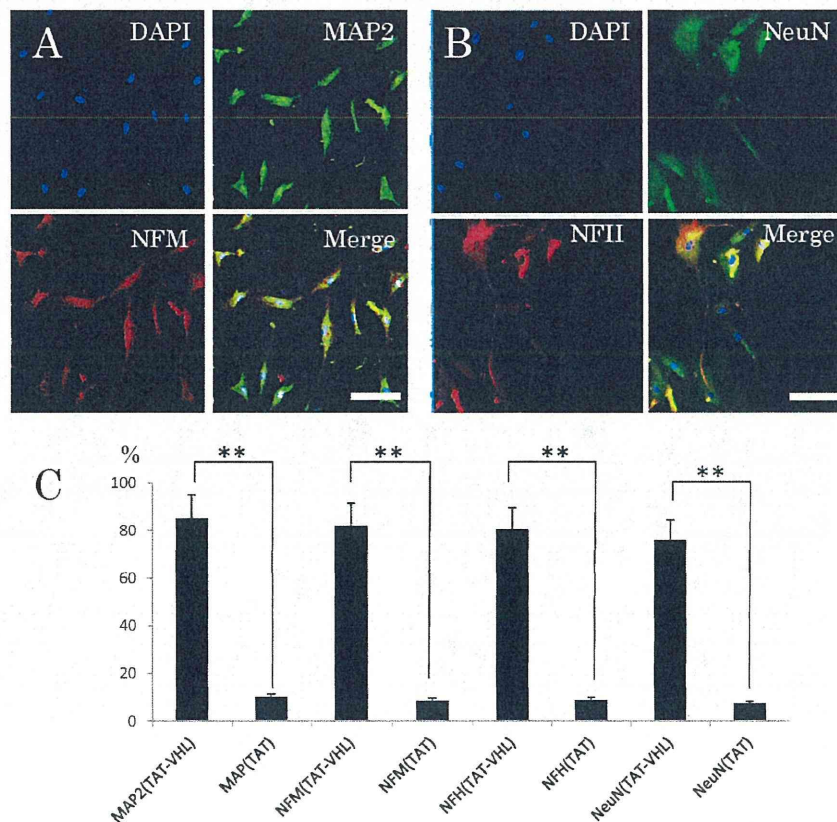
Figure 3. Fluorescence immunohistochemistry for skin, including epidermis and dermis, and epidermis only. (A) Triple fluorescence immunohistochemistry for expressions of nestin (green) and CD34 (red), and visualization of nuclei (blue) in the skin. Both nestin and CD34-co-expressing cells (arrow) are shown at the outer root sheath of hair follicles; (B) Triple fluorescence immunohistochemistry for expressions of nestin (green) and fibronectin (red), and visualization of nuclei (blue) in the skin. Both nestin and fibronectin-co-expressing cells (double arrows) are seen at the outer root sheath of hair follicles; (C) Double fluorescence immunohistochemistry for expression of keratin 15 (green) and visualization of nuclei (blue). Keratin 15 was identified in the hair follicle and keratinocyte layer; (D) Triple fluorescence immunohistochemistry of epidermis alone for nestin (green) and keratin 15 (red) and visualization of nuclei (blue). A nestin-expressing cell population was identified in the hair follicles. Keratin 15 was expressed in the outer layer. Scale bars = 50 μ m.



2.3. Neuronal Differentiation of Stem Cells after Intracellular Delivery of TAT-VHL Peptide

Neuronal differentiation of the stem cells was examined after the intracellular delivery of TAT-VHL peptide, which has been reported to have the ability to induce neuronal differentiation [25–27]. For the control, the neuronal differentiation of cells treated with TAT-peptide was also examined. At first, an *in vitro* study was done. Two days after the intracellular delivery of TAT-VHL peptide at a 1- μ M concentration in DMEM/F12 medium without growth or neurotrophic factors, phase-contrast microscopy and an immunocytochemical study were performed. Observation by phase-contrast microscopy showed that most cells after transfer of the TAT-VHL peptide into them grew neurite-like cellular processes ($78.3\% \pm 12.5\%$), whereas the control cells receiving TAT peptide extended significantly fewer of these processes ($18.6\% \pm 7.3\%$). In the immunocytochemical *in vitro* study, the TAT-VHL peptide-containing stem cells derived from the epidermis showed high expression of various neuronal markers (MAP2, Neurofilament-M, Neurofilament-H, and Tuj-1), whereas those containing the control TAT peptide showed low expression of these markers (Figure 4A–C).

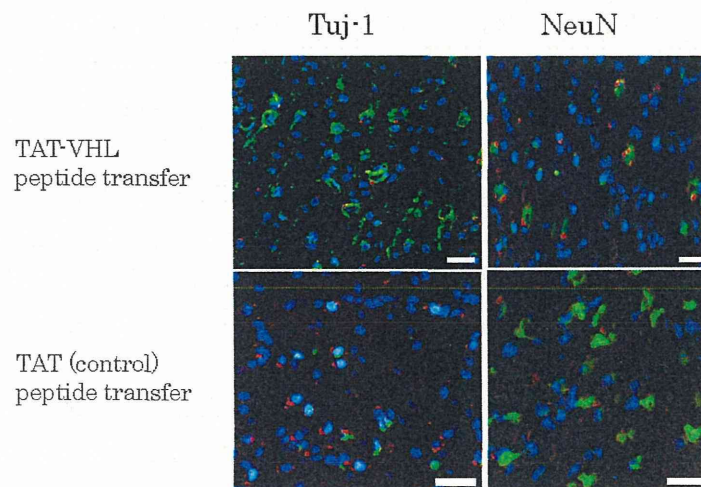
Figure 4. Fluorescence immunocytochemistry of the cultured stem cells after intracellular delivery of TAT-VHL peptide. (A) Triple fluorescence immunocytochemistry for expressions of MAP2 (green) and neurofilament-M (NFM, red) and visualization of nuclei (blue); (B) Triple fluorescence immunocytochemistry for NeuN (green) and neurofilament-H (NFH, red) and visualization of nuclei (blue); (C) Percentages of the TAT-VHL peptide- or TAT peptide- containing cells expressing MAP2, NFM, NFH or NeuN. The TAT-VHL peptide cells showed significantly higher expression of all 4 proteins (** $p < 0.001$). Scale bars = 30 μ m.



2.4. Implantation of Multipotent Nestin-Expressing Stem Cells into the Rodent Brain

TAT-VHL peptide-containing epidermal stem cells and control ones containing TAT peptide were pre-stained with red fluorescent PKH26, and separately implanted into Wistar rat brains. Three weeks later, after perfusion/fixation, the brains were frozen with liquid nitrogen and sectioned at 10 μm . Then, using anti-Tuj-1 and anti-NeuN antibodies, we performed an immunohistochemical study on these sections. Nuclei were stained with DAPI. The number of surviving implanted cells (red fluorescent PKH-pre-stained cells) among the TAT-VHL peptide-containing implanted cells ($20.4\% \pm 2.7\%$) was significantly greater than that of the TAT peptide-containing ones ($6.6\% \pm 0.8\%$, $p < 0.01$). In addition, PKH-pre-stained cells expressing Tuj-1 represented $38.8\% \pm 3.5\%$ of the TAT-VHL peptide-containing cell population, which percentage was significantly greater ($p < 0.01$) than the $9.3\% \pm 1.5\%$ found for the TAT peptide-containing one (Figure 5).

Figure 5. Fluorescence immunohistochemistry for rodent brain tissues implanted with peptide-transferred nestin-expressing stem cells pre-stained with red-fluorescent PKH26-PCL. Confocal immunohistochemical images showed expression of neuronal marker Tuj-1 (green) or NeuN (green). The nuclei were stained with DAPI (blue). PKH-pre-stained TAT-VHL peptide-containing cells showed significantly more expression of Tuj-1 and NeuN than did the pre-stained TAT peptide-containing ones ($p < 0.01$). Scale bar = 20 μm .



3. Discussion

In this report, we demonstrated the isolation of multipotent nestin-expressing stem cells derived from the epidermis of facial skin obtained from elderly humans (mean 69.1 years of age), and showed the neuronal differentiation of these cells when the TAT-VHL peptide was intracellularly delivered into them. The isolated cells showed sphere-forming ability and high expression of triple markers (fibronectin, nestin, and CD34), but very low expression of keratin 15 and NGFR p75. These findings are compatible with those on human hair follicle stem cells [2]. In addition, the results of our experiment to identify the niche of the stem cells suggested that the isolated nestin-positive stem cells originated from the outer sheath root of hair follicles. Murine multipotent nestin-expressing stem cells, derived from either the hair follicle bulge area or dermal papilla possess sphere-forming capacity [8]. Our

isolated multipotent nestin-positive cells also showed sphere-forming ability, which reflects self-renewing capacity [28], and was also found in the case of skin-derived neural crest stem cells [29] or skin-derived precursors [7]. Our isolated stem cells included the cells obtained from seven patients over 70 years of age (the oldest patient, 86 years old), and so our results indicate that skin-derived nestin-expressing follicle stem cells could be isolated even from patients over 70 years of age. In addition, our data clearly identified the niche of these stem cells; whereas most previous studies did not fully elucidated the stem cell niche and also never examined the expression of both fibronectin and CD34 simultaneously.

Multipotent nestin-expressing stem cells are promising as donor cells for the treatment of intractable neuronal diseases [20,30]. However, if these cells without neuronal differentiation are implanted, they scarcely survive or differentiate to functional neuronal cells, similar to the case of other stem cells. Therefore, before implantation for cell therapy of intractable neuronal diseases, such cells would be required to differentiate into neuronal cells. Our data showed that the stem cells treated *in vitro* with TAT-VHL peptide and implanted into rat brains survived and differentiated into neuronal marker-positive cells, even though the implantation was into another mammalian species, probably because the immune system in the central nervous system was not fully functional by the end of the short period of observation and because VHL protein contributes to the survival of implanted cells [31–33]. The elongin BC-binding site within the VHL protein is a domain that induces the neuronal differentiation of various stem cells [24–27], and so the intracellular delivery of the amino-acid sequence corresponding to this binding site would have brought about the neuronal differentiation of these somatic stem cells. In previous studies, it was shown that the intracellular delivery of TAT-VHL peptide induces not only *in vitro* neuronal differentiation of somatic stem cells but also *in vivo* neuronal differentiation and recovery from neuronal symptoms in neuronal disease models [25–27]. In addition, it was recently demonstrated that implantation of skin-derived precursors into which TAT-VHL peptide had been intracellularly delivered not only improved symptoms of Parkinson's model rats but also resulted in the secretion of dopamine in the rodent striatum [34]. Recently it was reported that implantation of human follicle pluripotent stem cells promotes regeneration from peripheral-nerve injury in nude mice [20,22]. We here showed that multipotent nestin-expressing stem cells isolated from the epidermis obtained from elderly humans differentiated into neuronal-marker positive cells even though xenografted into the brains of non-immune-deficient rats. Human leukocyte antigen (HLA)-type adaptable allograft implantation of nestin-expressing follicle stem cells into the central nervous system (CNS) might be tolerable without rejection and contribute to the promotion of CNS regeneration. Intractable neuronal diseases such as Parkinson's disease develop more frequently in elderly patients. Therefore, it is significant that multipotent stem cells derived from the epidermis can be obtained from elderly humans as well as from younger individuals. Basically, multipotent somatic stem cells do not transform into cancer cells, whereas iPS cells do; and the problem of malignant transformation of these cells has still not been solved. In practical use for human neuronal regeneration, multipotent somatic stem cells are considered to be superior to iPS cells. The mechanism of the neuronal differentiation of stem cells in response to the intracellular delivery of TAT-VHL peptide is not fully elucidated. It has been suggested that the binding of TAT-VHL peptide to elongin BC is competitive with the binding of elongin BC to elongin A, which is a critical reaction in messenger RNA elongation [35]. In addition, it was recently suggested that the VHL protein inhibits Stat3, which plays a decisive role in astroglial

differentiation [28]. This phenomenon might be related to the neuronal differentiation in response to the intracellular delivery of TAT-VHL peptide. The epidermis is an easily accessible source. Recently, truly pluripotent SSEA-3-positive MUSE cells were isolated from a skin fibroblast population by use of a cell sorter [36]. Although the population of somatic stem cells derived from the epidermis might contain MUSE cells, it may not be necessary to re-isolate MUSE cells from among such somatic stem cells since those stem cells themselves can differentiate into cells of the epithelial lineage in various organs. The neuronal differentiation method using TAT-VHL peptide is very simple because only the TAT-VHL peptide needs to be added to basic medium lacking serum, and it is also rapid compared with previously reported methods using various neurotrophic factors and other agents. Thus, we recommend the use of TAT-VHL for the neuronal differentiation of multipotent somatic stem cells.

4. Experimental Section

4.1. Cell Culture

Samples of human skin were sterilized with 70% ethanol for 1 min. Then, the skin was treated with dispase (concentration 1000 PU/mL) for 24 h at room temperature. Next, the epidermis was peeled off from the dermis, cut into small fragments with scissors, and digested with 0.1% trypsin for 30 min at 37 °C. Thereafter, the cells were filtered through a cell strainer (40- μ m-diameter holes) and subsequently cultured in medium containing epidermal growth factor (20 ng/mL), basic fibroblast growth factor (40 ng/mL), and 2% B27 supplement (Gibco-BRL, Grand Island, NY, USA) in DMEM/F12 (1:1; Gibco-BRL) in a 5% CO₂ incubator. The cells formed numerous spheres at 2–3 weeks after the start of the primary culture. Once the primary culture was 3–4 weeks old, the spheres were dissociated by pipetting; and the cells were subcultured every two weeks. For experiments, cells at the first or second subculture were used.

4.2. Identification of Niche of Multipotent Nestin-Expressing Stem Cells Derived from Human Epidermis

For identification of the niche of pluripotent sphere-forming stem cells derived from the epidermis, a part of the cut skin, which had been fixed with Mildform (Wako, Tokyo, Japan), was embedded in paraffin, sectioned at a 10- μ m thickness, and immunostained with anti-nestin antibody (BD Bioscience PharMingen, San Diego, CA, USA), anti-fibronectin antibody (Sigma, St. Louis, MO, USA), anti-CD34 antibody (Sigma) and anti-keratin 15 antibody (Acris Antibodies GmbH, Herford, Germany). As secondary antibodies, FITC-conjugated anti-mouse IgG monoclonal antibody (Sigma) and TRIC-conjugated anti-rabbit IgG polyclonal antibody were used. Finally, the nuclei were stained with DAPI (Molecular Probes, Eugene, OR, USA). Observation was performed by using a confocal fluorescence microscope (FV300, Olympus, Tokyo, Japan).

4.3. Immunocytochemical Characterization of Multipotent Stem Cells

After dissociation of the sphere-forming cells, characterization of the stem cells was performed immunocytochemically by using anti-nestin antibody, rabbit anti-fibronectin antibody (1:200; Sigma), anti-CD34 antibody, anti-NGFR p75 (Sigma), and anti-keratin 15 antibody (Acris Antibodies GmbH).

For examination of stem cell differentiation into certain cell types, anti-glial fibrillary acidic protein (GFAP) antibody (1:300; Dako, Glostrup, Denmark), anti-smooth muscle actin (SMA) antibody (1:200; Sigma), and anti-microtubule-associated protein (MAP)-2 (1:300; Sigma) were used. Immunoreactive cells were visualized by using either FITC-conjugated goat anti-mouse IgG (1:200; Sigma) or rhodamine-conjugated goat anti-rabbit IgG (1:150; Sigma) as secondary antibodies. To assess the frequency of different cell types in a given culture, we counted the number of cells immunopositive with a given antibody in 10 to 15 random non-overlapping visual fields (50–200 cells per field) in each experiment. At least three experiments were performed per condition. The degree of positivity was expressed as the ratio of immuno-positive cells to the total number of nuclei stained with DAPI.

4.4. Sphere-Forming Assay

The sphere formation assay was performed as follows [28]: Sphere-forming stem cells were dissociated into single cells by pipetting them continuously for 10 min. Then, after confirmation of their single-cell status and dilution up to 5 cells/mL, 200 μ L of the cell suspension was placed into each well of a 96-well plate (mean of 1 cell per well). Then, spheres ≥ 50 μ m in diameter in 1 plate were counted under observation by phase-contrast microscopy at 3 weeks after placement of the cells.

4.5. Induction of Neuronal Differentiation with TAT-VHL Peptide

By using the Fmoc (9-fluorenylmethyloxycarbonyl)-solid-phase method described previously [24], we chemically synthesized a peptide corresponding to the 157–171 amino-acid sequence of pVHL. The synthesized peptide was linked with the protein transduction domain (PTD) of the HIV-TAT protein (TAT-VHL peptide), thereby facilitating peptide entry into the cells. A control peptide composed of only the PTD of the TAT protein (TAT-peptide) was also synthesized. The sequences of these synthesized peptides were NH₂-YGRKKRRQRRRDTLKERCLQVVRSLVK-COOH for the TAT-VHL peptide and NH₂-YGRKKRRQRRR-COOH for the TAT one. The isolated stem cells were incubated in DMEM/F12, and 1 μ M TAT-VHL peptide or TAT peptide was delivered into the dissociated stem cells for neuronal differentiation. At first, an *in vitro* immunocytochemical study was performed. Three days after intracellular delivery of the TAT-VHL peptide in DMEM/F12 medium without growth or neurotrophic factors, the cells were observed under the phase-contrast microscope, and an immunocytochemical study was performed by using the following antibodies: anti-MAP2 antibody (1:200; Sigma), anti-tyrosine hydroxylase antibody (TH; 1:200; Merk Millipore, Billerica, MA, USA), and anti-neurofilament 200 antibody (1:200; Sigma). Immunoreactive cells were visualized by using either FITC-conjugated goat anti-mouse IgG (1:200; Sigma) or rhodamine-conjugated goat anti-rabbit IgG (1:150; Sigma) as secondary antibodies. In addition, DAPI (Molecular Probes) was used for counterstaining nuclei.

4.6. Implantation of Multipotent Stem Cells Derived from Epidermis

One hour after the TAT-VHL peptide had been transferred into the stem cells, the cells were stained with red-fluorescent PKH26PCL (Sigma), and implanted into the brains of eight-week-old Wistar rats (Charles River, Yokohama, Japan). Three weeks after the implantation, the rats were anesthetized with

Nembutal (200 mg/kg body weight) and perfused with periodate-lysine-paraformaldehyde solution. Their brains were subsequently dissected and postfixed in the same fixative for 2 h, cryopreserved in 30% sucrose for 12 h, and then embedded in Tissue Tek OCT compound (Sakura, Tokyo, Japan). Cryostat coronal sections of 14- μ m thickness were prepared and used for immunohistochemistry. For immunostaining, sections were incubated with primary antibody, *i.e.*, anti-NeuN antibody (1:200; Merk Millipore, Billerica, MA, USA) or anti-Tuj-1 antibody (1:200; R&D Systems, Minneapolis, MN, USA) for 1 h at room temperature. Immunoreactive cells were visualized by using either FITC-conjugated goat anti-mouse IgG (1:200; Sigma) or rhodamine-conjugated goat anti-rabbit IgG (1:150; Sigma) as secondary antibodies. In addition, DAPI was used for counterstaining nuclei.

4.7. Statistics

Results were expressed as the mean \pm standard deviation. For comparisons between values for groups, the Scheff test after the ANOVA test was used, with probabilities of less than 0.05 being considered significant (Statcel version 5.0/7.0, California, CA, USA).

4.8. Ethical Approval

This study was approved by the Ethics Committee of Yokohama City University in 2009, and the informed consent for this study was obtained from all of the patients.

5. Conclusions

In conclusion, we showed the isolation of multipotent nestin-expressing stem cells from the epidermis of facial skin of elderly humans and characterized these cells as being capable of sphere formation and strong expression of nestin, fibronectin, and CD34 but not of keratin 15. In addition, we identified the niche of these stem cells as being the outer root sheath of hair follicles and showed neuronal differentiation of these cells both *in vitro* and *in vivo* when VHL-peptide had been delivered into them. These multipotent stem cells derived from human epidermis are easily accessible and should be useful as donor cells for neuronal regenerative cell therapy.

Acknowledgements

This work was supported by grants from the Ministry of Education, Culture, Sports, Science, and Technology of Japan (Basic Research B, No. 23390353). The authors thank Akemi Miura for her technical assistance.

Conflict of Interest

The authors declare no conflict of interest.

References

1. Abbas, O.; Mahalingam, M. Epidermal stem cells: Practical perspectives and potential uses. *Br. J. Dermatol.* **2009**, *161*, 228–236.

2. Yu, H.; Fang, D. Isolation of a novel population of multipotent adult stem cells from human follicles. *Am. J. Pathol.* **2006**, *168*, 1879–1888.
3. Amoh, Y.; Mii, S.; Aki, R.; Hamada, Y.; Kawahara, K.; Hoffman, R.M.; Katsuoka, K. Multipotent nestin-expressing stem cells capable of forming neurons are located in the upper, middle and lower part of the vibrissa hair follicle. *Cell Cycle* **2012**, *11*, 3513–3517.
4. Amoh, Y.; Li, L.; Katsuoka, K.; Hoffman, R.M. Multipotent nestin-expressing hair follicle stem cells. *J. Dermatol.* **2009**, *36*, 1–9.
5. Sieber-Blum, M.; Grim, M.; Hu, Y.F.; Szeder, V. Pluripotent neural crest stem cells in the adult hair follicle. *Dev. Dyn.* **2004**, *231*, 258–269.
6. Hill, R.P.; Gledhill, K.; Gardner, A.; Higgins, C.A.; Crawford, H.; Lawrence, C.; Hutchison, C.J.; Owens, W.A.; Kara, B.; James, S.E.; *et al.* Generation and characterization of multipotent stem cells from established dermal cultures. *PLoS One* **2012**, *7*, e50742.
7. Toma, J.G.; McKenzie, I.A.; Bagli, D.; Miller, F.D. Isolation and characterization of multipotent skin-derived precursors from human skin. *Stem Cells* **2005**, *23*, 727–737.
8. Liu, F.; Uchugonova, A.; Kimura, H.; Zhang, C.; Zhao, M.; Zhang, L.; Koenig, K.; Duong, J.; Aki, R.; Saito, N.; *et al.* The bulge area is the major hair follicle source of nestin-expressing pluripotent stem cells which can repair the spinal cord compared to the dermal papilla. *Cell Cycle* **2011**, *10*, 830–839.
9. Uchugonova, A.; Duong, J.; Zhang, N.; König, K.; Hoffman, R.M. The bulge area is the origin of nestin-expressing pluripotent stem cells of the hair follicle. *J. Cell. Biochem.* **2011**, *112*, 2046–2050.
10. Amoh, Y.; Li, L.; Yang, M.; Moossa, A.R.; Katsuoka, K.; Penman, S.; Hoffman, R.M. Nascent blood vessels in the skin arise from nestin-expressing hair-follicle cells. *Proc. Natl. Acad. Sci. USA* **2004**, *101*, 13291–13295.
11. Uchugonova, A.; Hoffman, R.M.; Weinige, M.; Koenig, K. Watching stem cells in the skin of living mice noninvasively. *Cell Cycle* **2011**, *10*, 2017–2020.
12. Duong, J.; Mii, S.; Uchugonova, A.; Liu, F.; Moossa, A.R.; Hoffman, R.M. Real-time confocal imaging of trafficking of nestin-expressing multipotent stem cells in mouse whiskers in long-term 3-D histoculture. *In Vitro Cell. Dev. Biol. Anim.* **2012**, *48*, 301–305.
13. Amoh, Y.; Kanoh, M.; Niiyama, S.; Kawahara, K.; Sato, Y.; Katsuoka, K.; Hoffman, R.M. Human and mouse hair follicles contain both multipotent and monopotent stem cells. *Cell Cycle* **2009**, *8*, 176–177.
14. Brownell, I.; Guevara, E.; Bai, C.B.; Loomis, C.A.; Joyner, A.L. Nerve-derived sonic hedgehog defines a niche for hair follicle stem cells capable of becoming epidermal stem cells. *Cell Stem Cell* **2011**, *8*, 552–565.
15. Biernaskie, J.; Paris, M.; Morozova, O.; Fagan, B.M.; Marra, M.; Pevny, L.; Miller, F.D. SKPs derive from hair follicle precursors and exhibit properties of adult dermal stem cells. *Cell Stem Cell* **2009**, *5*, 610–623.
16. Amoh, Y.; Li, L.; Katsuoka, K.; Penman, S.P.; Hoffman, R.M. Multipotent nestin-positive, keratin-negative hair-follicle bulge stem cells can form neurons. *Proc. Natl. Acad. Sci. USA* **2005**, *102*, 5530–5534.

17. Klopper, J.E.; Tiede, S.; Brinckmann, J.; Reinhardt, D.P.; Meyer, W.; Faessler, R.; Paus, R. Immunophenotyping of the human bulge region: The quest to define useful *in situ* markers for human epithelial hair follicle stem cells and their niche. *Exp. Dermatol.* **2008**, *17*, 592–609.
18. Tiede, S.; Koop, N.; Klopper, J.E.; Fässler, R.; Paus, R. Nonviral *in situ* green fluorescent protein labeling and culture of primary, adult human hair follicle epithelial progenitor cells. *Stem Cells* **2009**, *27*, 2793–2803.
19. Garza, L.A.; Yang, C.C.; Zhao, T.; Blatt, H.B.; Lee, M.; He, H.; Stanton, D.C.; Carrasco, L.; Spiegel, J.H.; Tobias, J.W.; *et al.* Bald scalp in men with androgenetic alopecia retains hair follicle stem cells but lacks CD200-rich and CD34-positive hair follicle progenitor cells. *J. Clin. Invest.* **2011**, *121*, 613–622.
20. Amoh, Y.; Li, L.; Campillo, R.; Kawahara, K.; Katsuoka, K.; Penman, S.; Hoffman, R.M. Implanted hair follicle stem cells form Schwann cells that support repair of severed peripheral nerves. *Proc. Natl. Acad. Sci. USA* **2005**, *102*, 17734–17738.
21. Amoh, Y.; Li, L.; Katsuoka, K.; Hoffman, R.M. Multipotent hair follicle stem cells promote repair of spinal cord injury and recovery of walking function. *Cell Cycle* **2008**, *7*, 1865–1869.
22. Amoh, Y.; Kanoh, M.; Niiyama, S.; Hamada, Y.; Kawahara, K.; Sato, Y.; Hoffman, R.M.; Katsuoka, K. Human hair follicle pluripotent stem (hfPS) cells promote regeneration of peripheral-nerve injury: An advantageous alternative to ES and iPS cells. *J. Cell. Biochem.* **2009**, *107*, 1016–1020.
23. Kanno, H.; Saljoogue, F.; Yamamoto, I.; Hattori, S.; Yao, M.; Shuin, T.; U, H.-S. Role of the von Hippel-Lindau tumor suppressor protein during neuronal differentiation. *Cancer Res.* **2000**, *60*, 2820–2824.
24. Kanno, H.; Nakano, S.; Kubo, A.; Mimura, T.; Tajima, N.; Sugimoto, N. Neuronal differentiation of neural progenitor cells by intracellular delivery of synthetic oligopeptide derived from von Hippel-Lindau protein. *Protein Pept. Lett.* **2009**, *16*, 1291–1296.
25. Kubo, A.; Yoshida, T.; Kobayashi, N.; Yokoyama, T.; Mimura, T.; Nishiguchi, T.; Higashida, T.; Yamamoto, I.; Kanno, H. Efficient generation of dopamine neuron-like cells from skin-derived precursors with a synthetic peptide derived from von Hippel-Lindau protein. *Stem Cells Dev.* **2009**, *18*, 1523–1532.
26. Maeda, K.; Kanno, H.; Yamazaki, Y.; Kubo, A.; Sato, F.; Yamaguchi, Y.; Saito, T. Transplantation of von Hippel-Lindau peptide delivered neural stem cells promotes recovery in the injured rat spinal cord. *Neuroreport* **2009**, *20*, 1559–1563.
27. Yamazaki, Y.; Kanno, H.; Maeda, K.; Yoshida, T.; Kobayashi, N.; Kubo, A.; Yamaguchi, Y.; Saito, T. Engrafted VHL peptide-delivered bone marrow stromal cells promote spinal cord repair in rats. *Neuroreport* **2010**, *21*, 287–292.
28. Kanno, H.; Sato, H.; Yokoyama, T.; Yoshizumi, T.; Yamada, S. The VHL tumor suppressor protein regulates tumorigenicity of U87-derived glioma stem-like cells by inhibiting the JAK/STAT signaling pathway. *Int. J. Oncol.* **2013**, *42*, 881–886.
29. Wong, C.E.; Paratore, C.; Dours-Zimmermann, M.T.; Rochat, A.; Pietri, T.; Suter, U.; Zimmermann, D.R.; Dufour, S.; Thiery, J.P.; Meijer, D.; *et al.* Neural crest-derived cells with stem cell features can be traced back to multiple lineages in the adult skin. *J. Cell. Biol.* **2006**, *175*, 1005–1015.